Crack growth mechanism in granite specimens with non-persistent joints under punch shear through test

V. Sarfarazi[1], M. Fatehi Maraji[2]*, H. Haeri[3]

1- Dept. of Mining Engineering, Hamadan University of Technology, Hamadan, Iran
2- Dept. of Mining and Metallurgy, Yazd University, Yazd, Iran
3- Rahsazi & Omran Iran construction Company, Tehran, Iran

* Corresponding Author: *mohammad.fatehi@gmail.com*

Keywords	Abstract
punch-through shear test **rock bridge length** **rock bridge inclinations** **PFC2D**	Experimental and numerical methods (Particle Flow Code) were used to investigate the effect of echelon notches on the shear behavior of the joint's bridge area in granite. A punch-through shear test was used to model the granite cracks under shear loading. Granite samples with dimension of 20 mm×150 mm×40 mm were prepared in the laboratory. Within the specimen model and near the edges, four edge notches were provided. Nine different

configuration systems were prepared for notches. In these configurations, the length of each notch was taken as 3 cm, 4cm and 5 cm. Assuming a plane strain condition, special rectangular models were prepared with dimensions of 100 mm×100 mm using the particle flow code in two dimensions (PFC2D). Similar to those joints' configuration systems in the experimental tests, i.e. 9 models with different rock bridge lengths and different rock bridge joint angles were prepared. The axial load was applied to the punch through the central portion of the model. This testing showed that the failure process was mostly governed by the rock bridge length and the rock bridge angle. Shear strengths of the specimens were related to fracture pattern and failure mechanism of the discontinuities. It was shown that the shear behavior of discontinuities is related to the number of the induced tensile cracks which are increased by increasing the rock bridge angle. The strength of samples decreases with increasing the joint length. The failure pattern and failure strength are similar in both methods, i.e. the experimental testing and the numerical simulation.

1. INTRODUCTION

Design of rock engineering projects such as rock slopes and roadway excavations often requires the estimation of the strength and failure characteristics of the embedded rock mass that contains a large number of joints, or faults. These discontinuities have a great influence on the mechanical behavior of natural rocks. Under loading, new cracks will initiate from the pre-existing cracks and then propagate and coalesce with other cracks. During this process, propagation of cracks will contribute to further degradation of the strength and deformation modulus of the rock mass. (Wong [1]). These discontinuities and non-persistence cracks may have different geometries and bear complicated mechanical treatments affecting the stability and durability of the engineering structures. Many researchers have tried to study the mechanical behavior of discontinuities and cracks in rocks and concretes through the experimental tests carried out in the laboratories (Yang [2], Chen [3], De Bremaecker [4]). The crack initiation, crack propagation and their coalescences in the laboratory specimens containing a few open flaws under various loading conditions have been studied (Haeri [5-11], Sarfarazi [12-15] Sardemir [16], Wang [17]). However, in the most of these experimental tests, measuring the failure mechanism of the bridge area in the rock and concrete samples under various loading conditions was amongst the most difficult tasks. Therefore, several numerical methods such as

finite element methods (e.g. extended finite element method), boundary element methods (e.g. direct methods such as dual boundary element methods and indirect methods such as displacement discontinuity method) and finite difference methods (e.g. discrete element method) were developed to alternatively simulate most of the engineering fracture mechanics problems related to laboratory tests and rock engineering problems by considering the failure behavior and fracturing mechanism of non-persistent cracks, discontinuities and joints (Hosseini-nesab and Fatehi Marji, [18], Fatehi Marji [19-21]). The versatile discrete element method (DEM) originally developed by Cundall [22] is based on the explicit finite difference approach and proved to be an appropriate simulation technique for modelling the rock specimens and investigating the mechanical behaviors of geo-materials used in many rock engineering applications. In a particular version of the DEM, known as particle flow code in two dimensions (PFC2D) and three dimensions (PFC3D) the material consisting the rock specimens is envisioned as an assembly of elements representing the circular discs (for 2D) and spherical particles (for 3D), respectively. The micro-mechanical properties associated with the numerical simulations of modeled specimens with PFC3D need to be calibrated for a contact bonded particle model as explained by Kulattilake et al. [23]. They established a cracked rock model in their analyses, implementing the effect of closed flaws and studied the mechanical behavior of this cracked rock model assuming a uniaxial loading condition. They obtained a good relation between the micro and macro mechanical parameters of the modeled rock specimens. By removing some of the particles at the specified location within an assembly the open flaws can be produced for crack modeling (Ghazvinian [24]). The crack initiation and propagation process can be studied considering one, two and three open flaws in a specified modelled rock specimen as explained by Zhang [25]. In this procedure, most of the modelled crack propagation process simulated by the proposed numerical method are similar to those measured experimentally through laboratory tests. Another modeling procedure known as the smooth-crack model can be used to study the mechanical behavior of the cracked rock specimens using PFC2D. Bahaaddini et al. [26] used the smooth-crack model in a bonded particle algorithm to investigate the effect of crack geometry on the mechanism of the fracturing

process in rock masses containing non-persistent joints. In the present work, the specially designed specimens for a Punch Through Shear (PTS) test are modelled by the discrete element code to study the fracture mechanics of granite specimens. The numerical simulations are applied to the uniaxial compression and Brazilian tensile tests in the laboratory. The iterative semi-inverse modeling approach adopted in PFC3D is used to calibrate the shear strength and shear behavior of the bridge area. The experimental results measured by PTS tests are compared with the corresponding numerical results. This comparison shows that there are good agreements between these two sets of results. In this paper, both experimental and numerical methods were used to investigate the effect of echelon notches on the shear behavior of the joint's bridge area in granite specimens.

2. STAGES OF LABORATORY TESTS

2.1. Mechanical properties of samples

For determination of compressive strength of granite, a cylindrical specimen with a diameter of 54 mm and height of 108 mm was prepared (Kallimogiannis et al. [27]). Compressive strength of granite specimen was 207 MPa.

2.2. How to build specimens containing non - persistent joints

The granite specimens containing non-persistence joints are prepared in the laboratory. Dimension of samples was 20 cm *15 cm *4 cm. As shown in Figs. 1, nine rock bridge types with different angularities, i.e. 0° (Fig 1a), 55° (Fig 1b) and -55° (Fig 1c) were studied. For each rock bridge configuration, three joint lengths of 3 cm, 4 cm and 5cm were selected. Based on these rock bridge angularities, three different joint configurations have been defined, i.e., in the plane parallel joint system (Fig 1a); inside echelon joint system (Fig 1b) and outside echelon joint system (Fig 1c). In order to carry out loading on the specimens, that specimens are placed inside the uniaxial machine. Then stainless-steel blocks were placed between the specimen and the plates of the loading machine so that the punch shear loading condition was similar to that shown in Figs.1. The loading rate during the tests was kept as 0.005 mm/s.
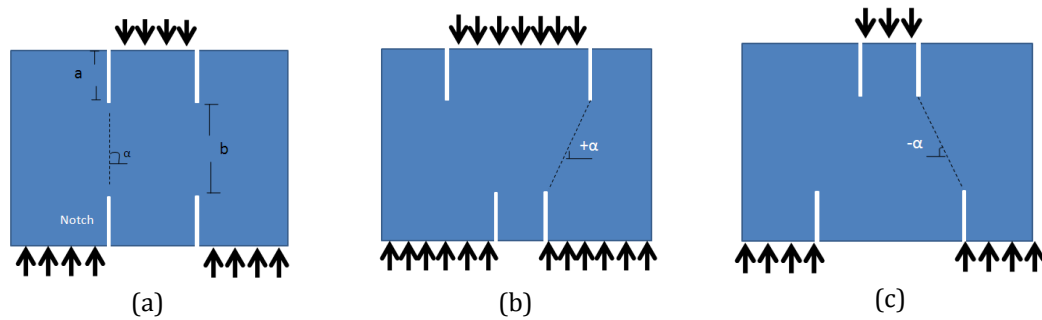
Fig. 1. The samples consisting edge joint with the rock bridge angle of, a) 0° b) 55° and c) -55°.

3. EXPERIMENTALLY OBSERVED FAILURE PATTERNS

3.1. Failure mechanism of samples

Fig. 2 shows the failure pattern of specimens containing non-persistent joint with rock bridge angle of 0°. When joint lengths were 6 cm (Fig. 2a), one tensile crack initiated from the upper joint tip and propagated vertically, and coalesced with lower tip of the lower joint. When joint lengths were 5 cm (Fig. 2b), again, one tensile crack initiated from the upper joint tip and propagated vertically till meet the lower tip of the lower joint. Nearly, the same phenomenon is repeated in the case of joints of 4 cm in length (Fig. 2c).
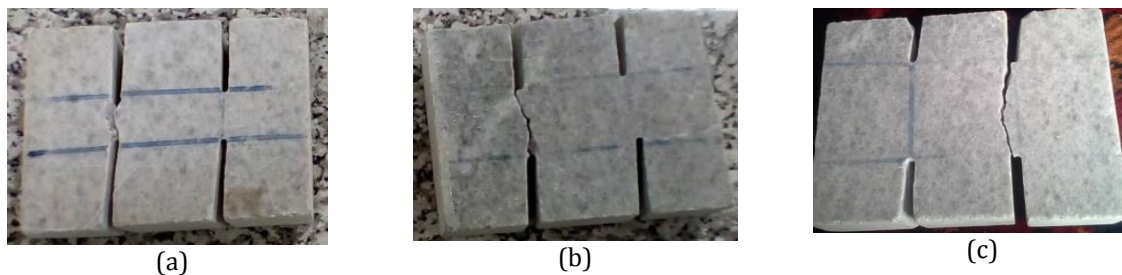
Fig. 2. The failure pattern of specimens with joint lengths of; a) 6cm, b) 5cm and c) 4cm for the bridge angularity of 0°.

Fig. 3 shows the failure pattern of specimens containing non-persistent joint with rock bridge angularity of 55°. When joint lengths were 6 cm (Fig. 3a), one tensile crack initiated from upper joint tip and propagated parallel to the loading axis till meet the lower boundary of samples. The same phenomena are repeated for the joint lengths of 5cm (Fig. 3b) and 6 cm (Fig. 3c), respectively.
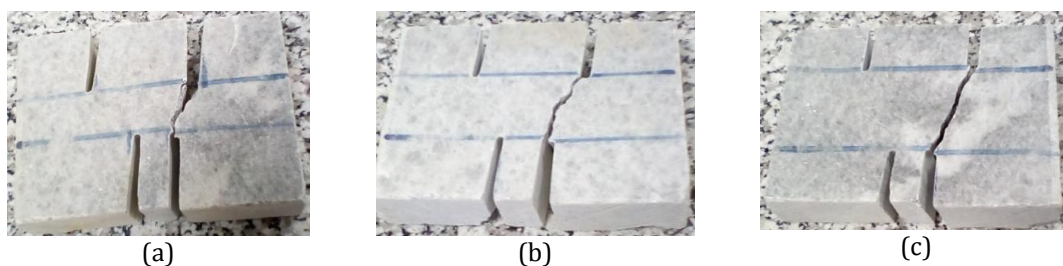
Fig. 3. Failure pattern of specimens with joint lengths of; a) 6cm, b) 5cm and c) 4cm for the bridge angularity of 55°.

Fig. 4 shows the failure pattern of specimens containing non-persistent joint with the rock bridge angularity of -55°. When joint lengths were 6 cm (Fig. 4a), one tensile crack initiated from the upper joint tip and propagated diagonally till coalesce with the lower tip of the lower joint. When joint lengths were 5 cm (Fig. 4b), again, one tensile crack initiated from the upper joint tip and propagated diagonally to meet the lower tip of the lower joint. The same scenario is repeated for the joint lengths of 4 cm as shown in Fig. 4c.

Finally, it can be concluded that when the rock bridge angle was 0°, the mixed mode failure (tensile/shear) occurs in the rock bridges. When the rock bridge angle was 55°, the pure tensile failure occurs in rock segments. On the other hand, the shear failure occurs in rock bridge when the rock bridge angle was -55°.
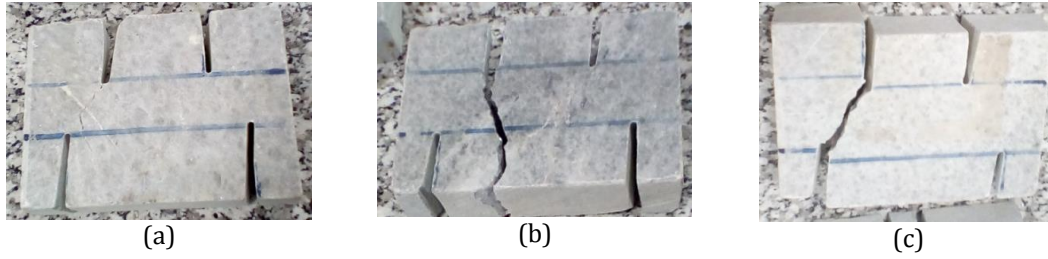
Fig. 4. Failure pattern of specimens with joint lengths of; a) 6cm, b) 5cm and c) 4cm for the bridge angularity of -55°.

3.2. Effect of joint length on the strength of samples

Fig. 5 shows the effect of joint length on the strength of samples for different joint configuration, i.e., in the plane parallel joint, inside echelon joint and outside echelon joint. The strength of samples decreases with increasing the joint length. Also, the outside echelon joint has a maximum value of strength while the inside echelon joint has the minimum value of tensile strength. In fact, rock bridge is under compressive force in the outside echelon joint while it is under tensile force in the inside echelon joint.
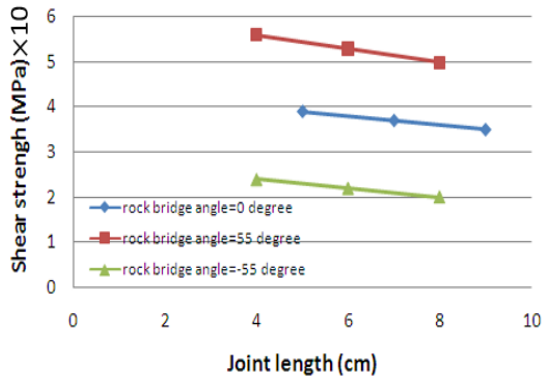
Fig. 5. Effect of joint length on the strength of samples for different joint configuration, i.e., in plane parallel joint (0 degree), inside echelon joint (55 degrees) and outside echelon joint (-55 degrees).

4. PFC SOFTWARE USED FOR THE NUMERICAL MODELING

PFC is a discrete element commercial software developed by the Itasca Consulting Group and has been widely used in rock mechanics [28]. PFC2D model represents a rock mass as an assemblage of circular disks with a finite thickness connected via cohesive and frictional bonds. A basic linear contact model describes the elastic relationship between the relative displacements and forces of disks at the point of contact, as shown in Fig. 6.
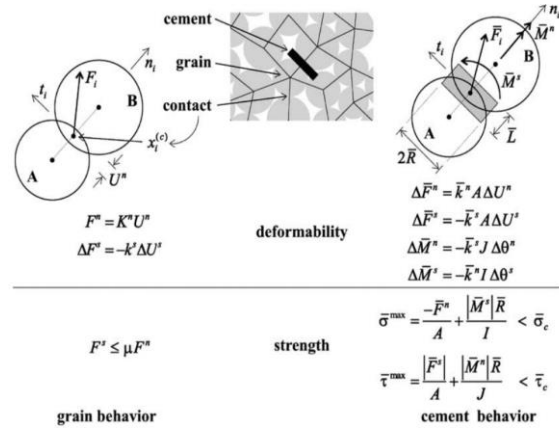
Fig. 6. The parallel bond model and the stress state between disks [28].

This model involves the contact normal force component, F_n, contact overlap, U_n, shear force increment, ΔF_s, and shear displacement increment, ΔU_s, and is given by:

$$F_n = k_n U_n \tag{1}$$

where k_n is the normal stiffness at the contact. The value of k_n is determined by the current contact stiffness model. Note that the normal stiffness, k_n, is a secant modulus in that it relates total displacement and force. The shear stiffness ks, on the other hand, is a tangent modulus in that it relates incremental displacement and force. The computation of the normal contact force from the geometry alone makes the code less prone to numerical drift and able to handle arbitrary placement of balls and changes in ball radii after a simulation has begun. The shear contact force is computed in an incremental fashion. When the contact is formed, the total shear contact force is initialized to zero. Each subsequent relative shear displacement increment results in an increment of elastic shear force that is added to the current value. The motion of the contact must be considered during this procedure.

The contact velocity can be resolved into normal and shear components with respect to the contact plane. Denoting these components by V_i^n and V_i^s for the normal and shear components,

respectively, the shear component of the contact velocity can be written as:

$$V_i^s = V_i - V_i^n = V_i - V_j n_j n_i \qquad (2)$$

The shear component of the contact displacement increment vector, occurring over a time step of Δt, is calculated by:

$$\Delta U_i^s = V_i^s \Delta t \qquad (3)$$

Then, the shear elastic force-increment vector can be calculated by:

$$\Delta F_s = -k_s \Delta U_s \qquad (4)$$

The frictional resistance of the contact is given by:

$$F_s \leq \mu F_n \qquad (5)$$

where μ is the friction coefficient between the disks. To simulate a relatively brittle rock-like material, it is necessary to cement these disks with a bonded model. This study uses the parallel bond model, which resists not only the contact forces, but also the moments between the disks at a cemented contact (Fig. 6). The function mechanism of the parallel bond model is described by:

$$\begin{aligned}
\Delta \bar{F}_n &= \bar{k}_n A \Delta U_n \\
\Delta \bar{F}_s &= \bar{k}_s A \Delta U_s \\
\Delta \bar{M}_n &= \bar{k}_s J \Delta \theta_n \\
\Delta \bar{M}_s &= \bar{k}_n J \Delta \theta_s
\end{aligned} \qquad (6)$$

where $\bar{F}_n$ and $\bar{F}_s$ are the force components about the center of the cemented-contact zone, $\bar{M}_n$ and $\bar{M}_s$ are the moments about the center of the cemented-contact zone, $\bar{k}_n$ and $\bar{k}_s$ are the normal and shear bond stiffness per unit area, respectively, θn and θs are the rotation angle components, and A, J, and I are the area, polar moment of inertia, and moment of inertia of the bond contact cross section, respectively. The strength of the cemented contact is then given by:

$$\begin{aligned}
\bar{\sigma}_{max} &= -\frac{-\bar{F}_n}{A} + \frac{|\bar{M}_s|\bar{R}}{I} < \bar{\sigma}_c \\
\bar{\tau}_{max} &= -\frac{-\bar{F}_s}{A} + \frac{|\bar{M}_n|\bar{R}}{J} < \tau_c
\end{aligned} \qquad (7)$$

where $\bar{R}$ is the radius of the bonded zone between the disks, t is the length of the bonded zone between the disks (Fig. 6), and $\bar{\sigma}_c$ and τ_c are the tensile and shear strength of the bond contact, respectively. Tensile cracks occur when the applied tensile stress exceeds the specified tensile strength of the parallel bond, $\bar{\sigma}_c$. Shear cracks occur when the applied shear stress exceeds the specified shear strength of the parallel bond, τ_c, either by rotation or by the shearing of the disks. The tensile strength at the contact immediately

drops to zero once the crack occurs, and the shear strength reduces to the residual friction strength [28].

4.1. Preparation and Calibration of the PFC2D Model for the rock samples

The standard process of generating a PFC2D assembly to represent a test model is used in this article (Ghazvinian [24]). The process involves: particle generation, packing the particles, isotropic stress installation (stress initialization), floating particle (floater) elimination and bond installation. However, the gravity effect did not need to be considered in this simulation because the specimens were small, and the gravity-induced stress gradient had a negligible effect on the macroscopic behavior. Both, the uniaxial compressive strength and Brazilian tests were carried out to calibrate the properties of particles and parallel bonds in this bonded particle model (Ghazvinian et al. [24]). Adopting the micro-properties listed in reference [15] and the standard calibration procedures (Ghazvinian [24]), a calibrated PFC particle assembly was created. Figs 7a and 7b show the experimental uniaxial compression test and numerical simulation, respectively. The compressive strength of numerical model was 208 MPa (to be the representative of granite sample). By comparing this data and the experimental results, a well matching is observed between the results of the experimental tests and the numerical simulation.

(a)   *(b)*
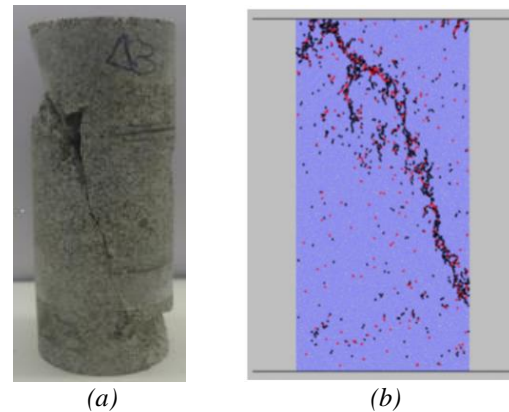
Fig. 7. a) Experimental compression test (Kallimogiannis et al. [27]), b) numerical compression test.

4.2. Numerical compressive Tests for the Non-Persistent Open Joint

After calibrating PFC2D, the punch shear tests for the non-persistent jointed rock samples were numerically simulated by creating a box model using the calibrated micro-parameters. The PFC specimen model had the dimensions of 100 mm ×

100 mm. A total of 13168 disks with a minimum radius of 0.27 mm was used to make up the box specimen. Two walls were created at the upper and lower of the model. The non-persistent joints were formed by deletion of bands of particles from the model. The opening of these notches (joints) is 1 mm (Figs. 8-10). In general, the models that each containing two non–persistent joints were constructed. The rock bridge angularities changed in three different values; i.e. 0° (Fig 8), 55° (Fig. 9) and -55° (Fig. 10). For each rock bridge configuration, the joint lengths were 2 cm, 3cm and 4cm. Based on the rock bridge angularities three different configurations were defined, i.e., in plate parallel joint (Fig. 8), inside echelon joint (Fig. 9) and outside echelon joints (Fig. 10). It should be noticed that these configurations are similar to those tested experimentally in the laboratory. The upper and lower walls of the model allowed to apply the uniaxial compressive force. This force was registered by taking the reaction forces on the upper wall.

4.3 The effects of joint configuration on the failure behavior of the modeled samples

In this model procedure, the fracture patterns of the modeled samples with different joint configurations are considered to study the effects of rock bridge angularities and join length on the fracturing process of the brittle materials in a punch through shear test.

4.3.1. Failure mechanism of the model with in-plane parallel joint configuration (rock bridge angularity of 0°)

In the failure mechanism of the modeled samples with different joint lengths (Fig. 8), the tensile wing cracks may initiate from the joint tip and propagate diagonally with respect to the direction of shear loading. Due to the low tensile strength of the modeled samples, the tensile cracks are the most dominant mode of failure compared to those in shear mode. At the peak shear loading condition, the branching occurs in the wing crack. Fig. 9 show the rose diagrams of the crack growth patterns for different joint lengths. As shown in these figures, the angles of micro cracks varied from 75 to 105 degrees.

(a)   (b)   (c)
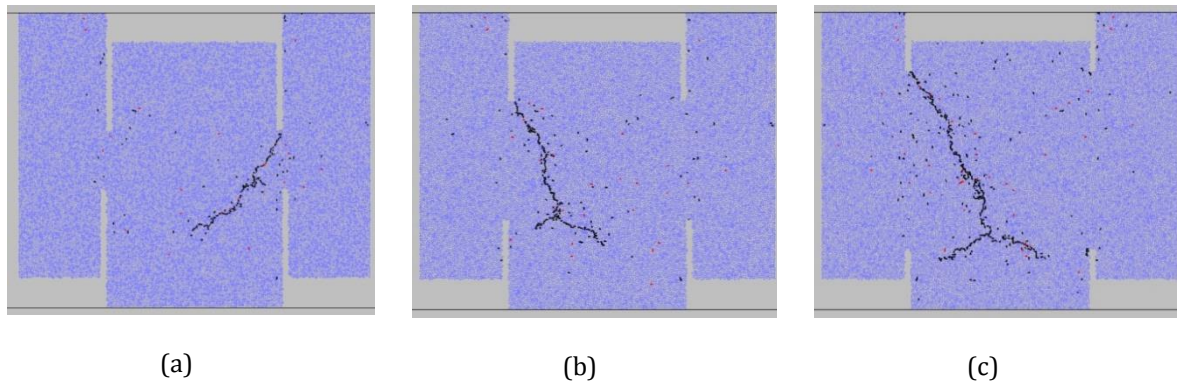
Fig. 8. In-plane parallel joint configuration, joints lengths were a) 4cm, b) 3cm and c) 2cm.

(a)   (b)   (c)
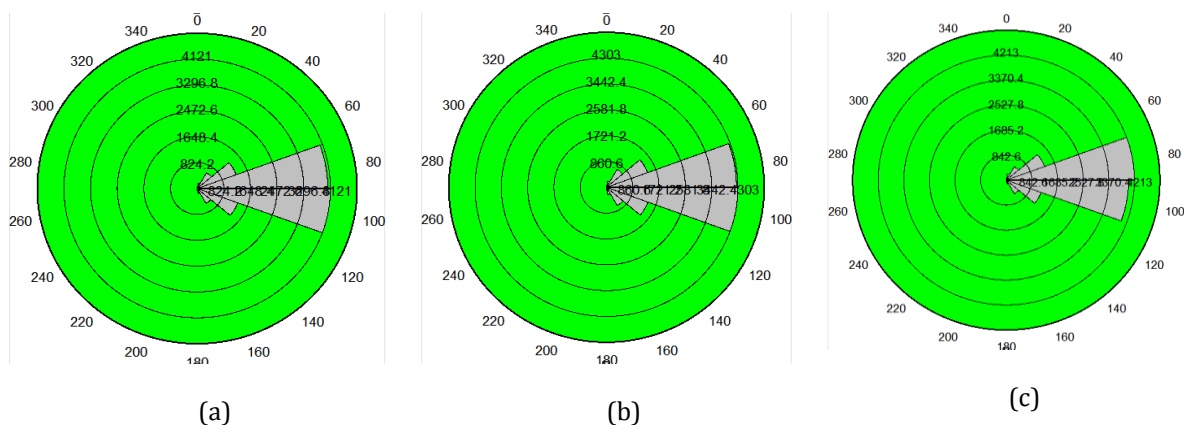
Fig. 9. Rose diagrams of crack growth for in-plane parallel joint configuration; joints lengths were a) 4cm, b) 3cm and c) 2cm.

4.3.2. Failure mechanism of the model with inside echelon joint configuration (rock bridge angularity of 55°)

In the failure mechanism of the modeled samples with different inside echelon joint length (Fig. 10), the tensile wing cracks may initiate from the joint tip and propagate diagonally with respect

to the direction of shear loading till coalesce with another joint tip. Again, in this case, the tensile cracks are also the most dominant mode of failure compared to those in shear mode. Fig 11 shows the rose diagrams of crack growth in the modeled samples. In this case, the angles of micro cracks varied from 75 to 105 degrees.

(a)　　　　　　　　　(b)　　　　　　　　　(c)
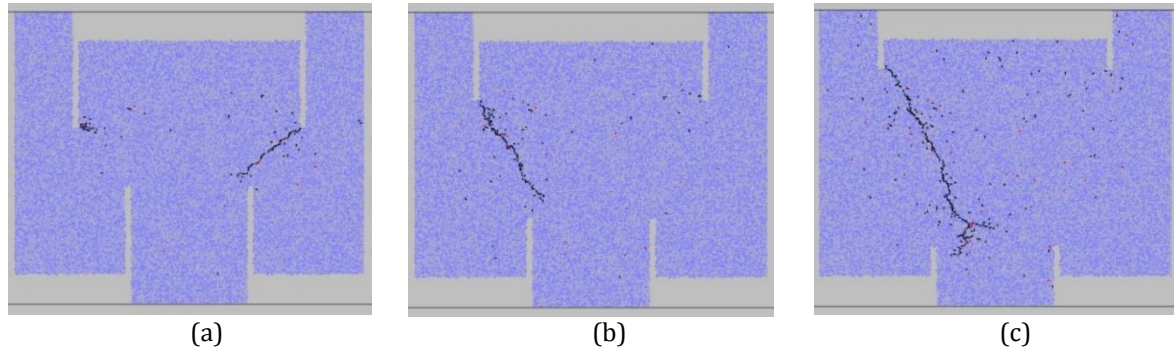
Fig. 10. Inside echelon joint configuration, joints lengths are a) 4cm, b) 3cm and c) 2cm.

(a)　　　　　　　　　(b)　　　　　　　　　(c)
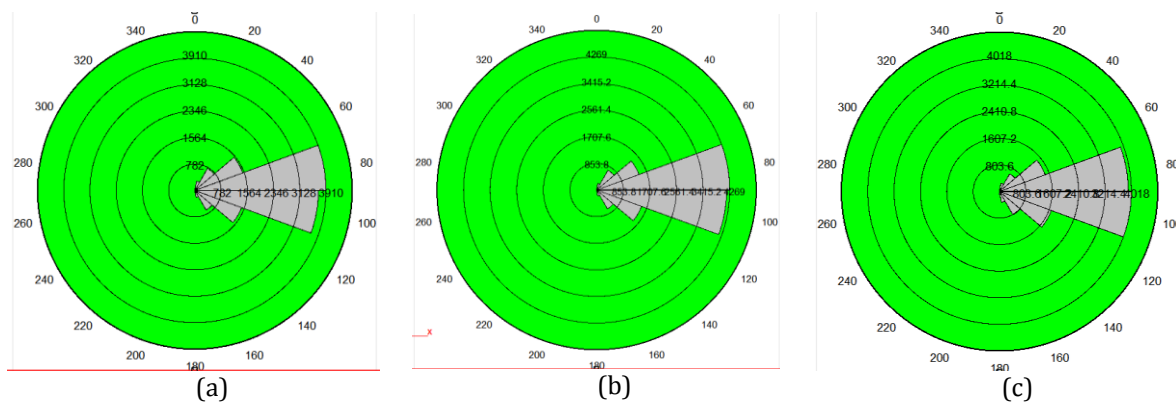
Fig. 11. Rose diagrams of crack growth for inside echelon joint configuration; joints lengths are a) 4cm, b) 3cm and c) 2cm.

4.3.3. Failure mechanism of the out-side echelon joint configuration model (rock bridge angularity of -55°).

In the failure mechanism of the modeled samples with different out-side echelon joint length (Fig. 12), the tensile wing cracks may initiate from the joint tip and propagate diagonally with respect to the direction of shear loading. Due

to the low tensile strength of the modeled samples, the tensile cracks are the most dominant mode of failure compared to those in shear mode. Fig. 13 shows Ross diagrams of crack growth. From Fig. 13, the angles of micro cracks varied from 75 to 105 degree.

(a)　　　　　　　　　(b)　　　　　　　　　(c)
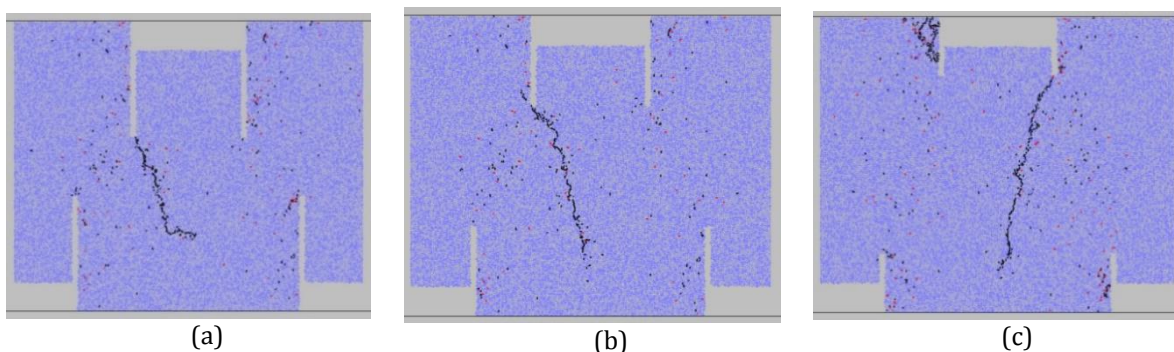
Fig. 12. Outside echelon joint configuration; joints lengths are a) 4cm, b) 3cm and c) 2cm.

(c)   (b)   (a)
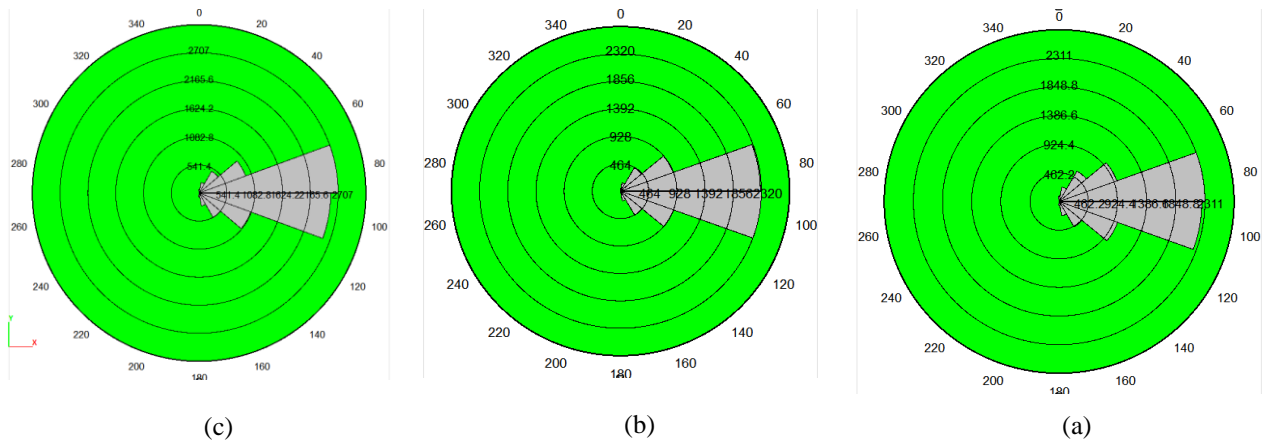
Fig. 13. Rose diagrams of crack growth for outside echelon joint configuration; joints lengths are a) 4cm, b) 3cm and c) 2cm.

By comparison, between Figs 2-4 and Figs 8, 10 and 12, it can be concluded that failure pattern is nearly similar in both of the experimental test and numerical simulation. In fact, when rock bridge angle was 0°, in-plane failure occurs in experimental tests (Fig 2) but the branching occurs in numerical simulation (Fig. 8). This is due to stress redistribution effect in numerical models. When the rock bridge angle was 55°, diagonal tensile failure occurs in both of the experimental tests (Fig. 3) and numerical simulation (Fig. 10). When the rock bridge angle was -55°, diagonal tensile failure occurs in both of the experimental tests (Fig 4) and numerical simulation (Fig. 12). In this configuration, newborn tensile cracks go through the model because of lower tensile strength of material related to its shear strength.

4.4 The The effect of joint length on the strength of samples

Fig. 14 shows the effect of joint length on the strength of modeled samples considering three different joint configurations, i.e., in the plane parallel joint, inside echelon joint and outside echelon joint. The strength of samples decreases with increasing the joint length. Also the outside echelon joint configuration has the maximum value of strength while the inside echelon joint has the minimum. In fact, rock bridge is under compressive force in the outside echelon joint configuration (Fig 12) while it is under tensile force in the inside echelon joint configuration (Fig 10).
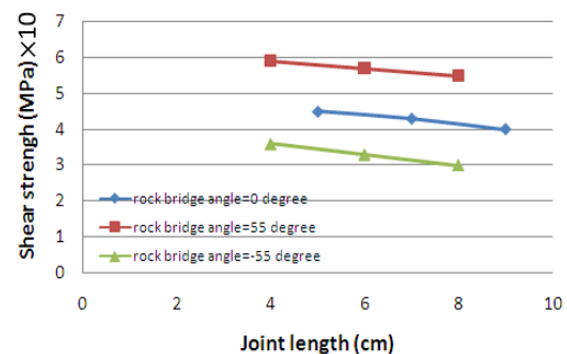
Fig. 14. the effect of joint length on the strength of models for different joint configurations; i.e. in plane parallel joint, inside echelon joint and outside echelon joint.

Comparing Fig 5 with Fig 14, it can be concluded that failure strength is nearly similar in both experimental test and numerical simulation. The difference between the numerical results with those obtained experimentally is about 5%.

5. CONCLUSIONS

Experimental and Particle Flow Code methods were used to investigate the effect of echelon notches on the shear behavior of the joint's bridge area in granite specimens. Based on the experimental and numerical results obtained in this study, the following main conclusions can be stated:

- In all samples, cracks were initiated from joint tips and propagated diagonally till coalescence with opposite joint tips.
- Tensile crack was smooth without pulverized material.
- Shear cracks have step shape with pulverized material.
- When the rock bridge angle was 0°, the mixed mode failure (tensile/shear) occurs in rock bridges. When the rock bridge angle was 55°, the pure tensile

failure occurs in rock segments and the shear failure occurs in rock bridge when the rock bridge angle was -55°.

- The angles of induced micro cracks varied from 75 to 105 degrees.
- The strength of samples decreases with increasing the joint length. Also the outside echelon joint has the maximum value of strength while the inside echelon joint has the minimum value of tensile strength.
- Failure patterns are similar in both of the experimental test and numerical simulation model. A bit difference between the experimental failure pattern and its corresponding numerical one was due to grain shape. Because in numerical simulation the grain shape was assumed to be a circular while in the physical granite samples, the grain shape may not be a circular for all grains.
- The overall failure strength of the granite samples is similar in both experimental test and numerical simulation.

REFERENCES

[1]   Wong, R.H.C. (1998), "Crack coalescence in a rock-like material containing two cracks", Int. J. Rock Mech. Min. Sci., 35(2), 147-164.

[2]   Yang, S.T., (2011), "Influence of local fracture energy distribution on maximum fracture load of three point-bending notched concrete beams", Eng. Fract. Mech., 78, 3289-99.

[3]   Chen, X., Liao, Z.H. (2013), "Cracking process of rock mass models under uniaxial compression", J. Central South Univ., 20(6), 1661-1678.

[4]   De Bremaecker, J.C. (2004), "Numerical models of shear fracture propagation", Engineering Fracture Mechanics., 71(15), 21612178.

[5]   Haeri, H., Marji, MF. (2015), "Experimental and Numerical Simulation of the Microcrack Coalescence Mechanism in Rock-Like Materials" strength of materials 47 (5), 740-754.

[6]   Haeri, H. and Sarfarazi, V. (2016a), "The effect of micro pore on the characteristics of crack tip plastic zone in concrete", Comput. Concrete, 17(1), 107-12.

[7]   Haeri, H. and Sarfarazi, V. (2016b), "The effect of non-persistent joints on sliding direction of rock slopes", Comput. Concrete, 17(6), 723-737.

[8]   Haeri, H. and Sarfarazi, V. (2016c), "The deformable multi-laminate for predicting the elasto-plastic behavior of rocks", Comput. Concrete, 18, 201-214.

[9]   Haeri, H., and Fatehi Marji, M. (2015), "Fracture analyses of different pre-holed concrete specimens under compression", Acta Mech Sin, 31(6), 855-870.

[10]   Haeri, H., Sarfarazi, V. (2016d), "Experimental study of shear behavior of planar non-persistent joint", Comput. Concrete, 17(5), 639-653.

[11]   Haeri, H., Shahriar, K., Marji, M.F. (2013), "Modeling the propagation mechanism of two random micro cracks in rock Samples under uniform tensile loading", 13th International Conference on Fracture, Beijing, China.

[12]   Sarfarazi, V. and Haeri, H., (2016a), "Effect of number and configuration of bridges on shear properties of sliding surface", J. Min. Sci., 52(2), 245-257.

[13]   Sarfarazi, V., (2016b), "A new approach for measurement of anisotropic tensile strength of concrete", Adv. Concrete Constr., 3(4), 269-284.

[14]   Sarfarazi, V., (2014), "Numerical simulation of the process of fracture of Echelon rock joints", Rock Mech. Rock Eng., 47(4), 1355-1371.

[15]   Sarfarazi, V., (2016), "The effect of non-persistent joints on sliding direction of rock slopes", Comput. Concrete, 17(6), 723-737.

[16]   Sardemir, M. (2016), "Empirical modeling of flexural and splitting tensile strengths of concrete containing fly ash by GEP", Comput. Concrete, 17(4), 489-498.

[17]   Wang, X., Zhu, Z., (2017), "Study of rock dynamic fracture toughness by using VB-SCSC specimens under medium-low speed impacts", Eng. Fract. Mech., 181, 52-64.

[18]   Hosseini_Nasab, H., Fatehi Marji M. (2007) A semi-infinite higher-order displacement discontinuity method and its application to the quasistatic analysis of radial cracks produced by blasting, Journal of Mechanics of Materials and Structures 2 (3), 439-458.

[19]   Marji, MF. (2013) On the use of power series solution method in the crack analysis of brittle materials by indirect boundary element method, Engineering Fracture Mechanics 98, 365-382.

[20]   Marji, MF. (2014) Numerical analysis of quasi-static crack branching in brittle solids by a

modified displacement discontinuity method, International Journal of Solids and Structures 51 (9), 1716-1736.

[21]   Marji, MF. (2015) Simulation of crack coalescence mechanism underneath single and double disc cutters by higher order displacement discontinuity method, Journal of Central South University 22 (3), 1045-1054.

[22]   Cundall, P.A. (1979), "A discrete numerical model for granular assemblies", Geotechnique, 29(1), 47-65.

[23]   Kulatilake, P.H.S.W., Malama, B. (2001), "Physical and particle flow modeling of jointed rock block behavior under uniaxial loading", Int. J. Rock Mech. Min. Sci., 38(5), 641-657.

[24]   Ghazvinian, A., Sarfarazi, V., (2012), "A study of the failure mechanism of planar non-persistent open joints using PFC2D", Rock Mech. Rock Eng., 45(5), 677-693.

[25]   Zhang, X.P (2013), "Crack initiation, propagation and coalescence in rock-like material containing two flaws: a numerical study based on bonded-particle model approach", Rock Mech. Rock Eng., 46(5), 1001-1021.

[26]   Bahaaddini, M., Sharrock, G. (2013), "Numerical investigation of the effect of joint geometrical parameters on the mechanical properties of a non-persistent jointed rock mass under uniaxial compression", Computer. Geotechnic., 49, 206-225.

[27]   Kallimogiannis V., Saroglou H., (2017), Study of Cracking Process in Granite, Procedia Engineering   191, 1108 – 1116.

[28]   D. O. Potyondy and P. A. Cundall, (2004) "A bonded-particle model for rock," International Journal of Rock Mechanics and Mining Sciences, 41(8): 1329–1364.